TWO-TIME-SCALE TURBULENCE MODELLING OF A FULLY-PULSED AXISYMMETRIC AIR JET

K. Bremhorst
Department of Mechanical Engineering,
The University of Queensland
Brisbane, Queensland 4072, Australia
k.bremhorst@uq.edu.au

T.J. Craft, B.E. Launder
Department of Mechanical, Aerospace and Manufacturing Engineering,
UMIST
Manchester M60 1QD, UK
tim.craft@umist.ac.uk, brian.launder@umist.ac.uk

ABSTRACT

Computations of a fully pulsed air jet are presented using a two-scale eddy-viscosity based scheme and an advanced stress transport model. Like other single scale models, the stress transport scheme fails to capture many features of the flow. In contrast, the two-scale model, however, does reproduce some important elements of the flow development. Further examination of the model performance suggests that its success is due in part to the implied spectral non-equilibrium, but also to the particular form of source terms employed in the transport equation for the turbulence energy transfer rate.

INTRODUCTION

Pulsed air jets have been shown by Bremhorst & Harch (1979) to result in greater entrainment of the ambient air compared to steady jets with the same mass flow rate. They are thus of particular interest in a number of chemical and combustor mixing applications where the length of the mixing zone is limited.

The steady axisymmetric jet in stagnant surroundings is itself known to be a difficult flow to predict. Two-equation eddy-viscosity models and even standard stress transport closures both give spreading rates for this flow that are some 30% too high if coefficients are tuned to predict correctly the plane 2-dimensional jet and other 'strong' free shear flows. Experiments and subsequent computational comparisons of the fully-pulsed[1] axisymmetric jet by workers at the University of Queensland (see Bremhorst & Gehrke, 2000; Nordsveen & Bremhorst, 1998; Graham & Bremhorst, 1993) have shown that this unsteady flow poses yet further modelling challenges. Even if the sink coefficient of the ε equation is adjusted to give the correct spreading rate of the axisymmetric steady jet, the models tested so far, whether at eddy viscosity or stress transport level, have failed to capture important dynamic features of the pulsed jet. Graham & Bremhorst (1993), for example, showed that with a k-ε scheme, the destruction term in the ε equation had to be increased by around 20% at a downstream position where the jet begins to change from being pulse-dominated to exhibiting a more steady behaviour in order to capture at least some of the measured development features.

The present contribution focuses on two rather different closure models. These are the two-component-limit (TCL) stress-transport model (see, for example, Craft et al, 1996) and the original two-time-scale approach of Hanjalić et al (1980). Unlike nearly all other approaches, these models both succeed in resolving correctly the so-called axisymmetric/plane jet anomaly. They achieve their success by different model features, however: the TCL model uses stress invariants in the ε equation and a complex pressure-strain model that is exact in the two-component limit, whilst the two-time-scale model makes the ε equation highly sensitive to normal strains and splits the energy spectrum into low and medium wave-number parts, solving k and ε equations for each part.

The following sections describe the models investigated, and outline some details of the numerical solution method. The model predictions of the pulsed jet flows are then discussed, and the various features of the models are analysed in an attempt to identify which are the crucial elements needed to capture these unsteady jet flows.

[1] Fully pulsed implies that the minimum velocity through the cycle falls to zero

TURBULENCE MODELLING

TCL Stress Transport Scheme

The TCL model is algebraically very lengthy and is not reproduced here. Its length, however, arises from analysis rather than simply the addition of many empirical terms, and ensures that the model returns the correct behaviour of the stresses in the limit as one fluctuating velocity component vanishes. In addition to a non-linear pressure-strain model designed to satisfy this limit, the scheme also employs an ε equation of the usual form:

$$\frac{D\varepsilon}{Dt} = c_{\varepsilon 1}\frac{\varepsilon P_k}{k} - c_{\varepsilon 2}\frac{\varepsilon^2}{k} + \frac{\partial}{\partial x_k}\left[c_\varepsilon \frac{k\overline{u_k u_l}}{\varepsilon}\frac{\partial \varepsilon}{\partial x_l}\right] \quad (1)$$

although the coefficient $c_{\varepsilon 1}$ is reduced from its standard value of 1.44 to unity, whilst $c_{\varepsilon 2}$ is sensitized to stress anisotropy by making it a function of the anisotropy invariants:

$$c_{\varepsilon 2} = \frac{1.92}{1 + 0.7A_2^{1/2}A} \quad (2)$$

where $A_2 = a_{ij}a_{ij}$, $A_3 = a_{ij}a_{jk}a_{ki}$, $a_{ij} = \overline{u_i u_j}/k - 2/3\delta_{ij}$ and $A = 1 - (9/8)(A_2 - A_3)$.

Besides the cited reference in the Introduction, the TCL scheme is presented *inter alia* in Launder & Li (1994) and Craft & Launder (2001), and has been shown to return superior results to the basic linear stress transport model in a variety of shear and buoyancy dominated flows.

Two-Scale Eddy-Viscosity Scheme

The two-time-scale model uses idealized spectral partitioning to separate the turbulence spectrum into a production range, a transfer range and a dissipation range. The turbulent kinetic energy, k_P, is produced in the production range. Energy leaves this range by being broken down to smaller eddies; that is, there is an energy transfer across the spectrum into the transfer range at a rate ε_P. Although no mean-strain production occurs in the transfer range, it does contain turbulent kinetic energy which can diffuse, convect and flow at a rate ε_T into the dissipation range. The latter contains no turbulent kinetic energy and consequently ε_T becomes the dissipation rate, ε. In an equilibrium flow, spectral transfer processes are assumed to be slow enough so that $\varepsilon_P = \varepsilon_T = \varepsilon$. The two-time-scale model equations proposed by Hanjalić et al (1980) are:

$$\frac{Dk_P}{Dt} = -\overline{u_i u_j}\frac{\partial U_i}{\partial x_j} - \varepsilon_P + D_{k_P} \quad (3)$$

$$\frac{Dk_T}{Dt} = \varepsilon_P - \varepsilon_T + D_{k_T} \quad (4)$$

$$\frac{D\varepsilon_P}{Dt} = -C_{P1}\frac{\varepsilon_P}{k_P}\overline{u_i u_j}\frac{\partial U_i}{\partial x_j} - C_{P2}\frac{\varepsilon_P^2}{k_P} + D_{\varepsilon_P} + C'_{P1}k_P\frac{\partial U_l}{\partial x_m}\frac{\partial U_i}{\partial x_j}\varepsilon_{lmk}\varepsilon_{ijk} \quad (5)$$

$$\frac{D\varepsilon_T}{Dt} = C_{T1}\frac{\varepsilon_P\varepsilon_T}{k_T} - C_{T2}\frac{\varepsilon_T^2}{k_T} + D_{\varepsilon_T} \quad (6)$$

The various diffusion terms are modelled as

$$D_\phi = 0.09\frac{\partial}{\partial x_j}\left(\frac{kk_P}{\varepsilon_P}\frac{\partial \phi}{\partial x_j}\right) \quad (7)$$

where ϕ stands for k_P, k_T, ε_P or ε_T and k denotes the total turbulent kinetic energy, $k = k_P + k_T$. Finally the Reynolds stresses are obtained from the linear eddy viscosity expression:

$$\overline{u_i u_j} = -0.09\frac{kk_P}{\varepsilon_P}\left(\frac{\partial U_i}{\partial x_j} + \frac{\partial U_j}{\partial x_i}\right) + 2/3k\delta_{ij} \quad (8)$$

The same values of all coefficients were retained as in the original paper (including functional dependencies of two of the coefficients on the dimensionless ratios k_P/k_T and $\varepsilon_P/\varepsilon_T$), and these are given in Table 1. In addition to the partitioning of the turbulence spectrum, the model is also seen to contain two types of generation terms for ε_P in equation (5). These are designed to produce a greater energy transfer rate when there is significant irrotational straining compared to that found in a simple shear flow. Hanjalić et al applied the model to a strongly strained contraction flow and showed that the spectral lags introduced by it lead to significantly better predictions than when a single-scale model was employed.

Subsequent development and further applications of a two-scale model have been reported by, *inter alia*, Mataoui et al (2001). However, when applying this later form to the present case a variety of numerical stability problems were encountered. The present explorations have thus been based around the earlier scheme of Hanjalić et al, as described above.

Table 1: Model coefficients in the Hanjalić et al (1980) two-scale scheme.

C_{P1}	C'_{P1}	C_{P2}
2.2	-0.11	$1.8 - 0.3\frac{k_P/k_T-1}{k_P/k_T+1}$

C_{T1}	C_{T2}
$1.08\varepsilon_P/\varepsilon_T$	1.15

NUMERICAL TREATMENT

Computations have been performed with a suitably modified version of the elliptic code STREAM (Lien & Leschziner, 1994). This is a finite volume based solver, employing a collocated storage arrangement. The SIMPLE pressure correction is used, with Rhie & Chow (1983) interpolation for the mass fluxes across cell faces, and the convective terms are discretized via the UMIST scheme

(Leschziner & Lien, 1994). An expanding mesh was employed, with 240 axial cells extending 100 diameters downstream, and 60 radial nodes extending far enough from the axis to capture all the axial flow. For the pulsed jet calculations, 500 time steps were used to cover each pulse. Tests with finer grids and smaller time steps confirmed the grid-independency of the solutions.

To match the experiments of Bremhorst & Gehrke (2000), most of the calculations have been performed for a jet pulsed at 10Hz, with a 1:2 ratio of on to off time. During the on period, a sine squared variation of the inlet velocity was prescribed, following Nordsveen & Bremhorst (1998):

$$U_{in}(t) = 2U_b \frac{\tau_o}{\tau_c} \sin^2(t\pi/\tau_c)$$

where τ_o is the time of one cycle, τ_c the "on" time, and U_b the mean inlet velocity. The Reynolds number of the flow, based on U_b and inlet jet diameter was 30,000, and the corresponding Strouhal number was 0.0035.

RESULTS

Steady Axisymmetric Jet

Table 2 shows the spreading rates for the steady axisymmetric jet predicted by the standard k-ε, TCL stress transport and two-scale model of Hanjalić et al (labelled HLS). As previously noted, the k-ε model significantly overpredicts the spreading rate, whilst the other two schemes predict broadly the correct level (it should be noted that all three schemes produce the correct spreading rate for the corresponding plane jet).

Table 2: Steady axisymmetric jet spreading rates.

	$dy_{1/2}/dx$
Experiment	0.093
k-ε model	0.112
TCL model	0.096
HLS model	0.092

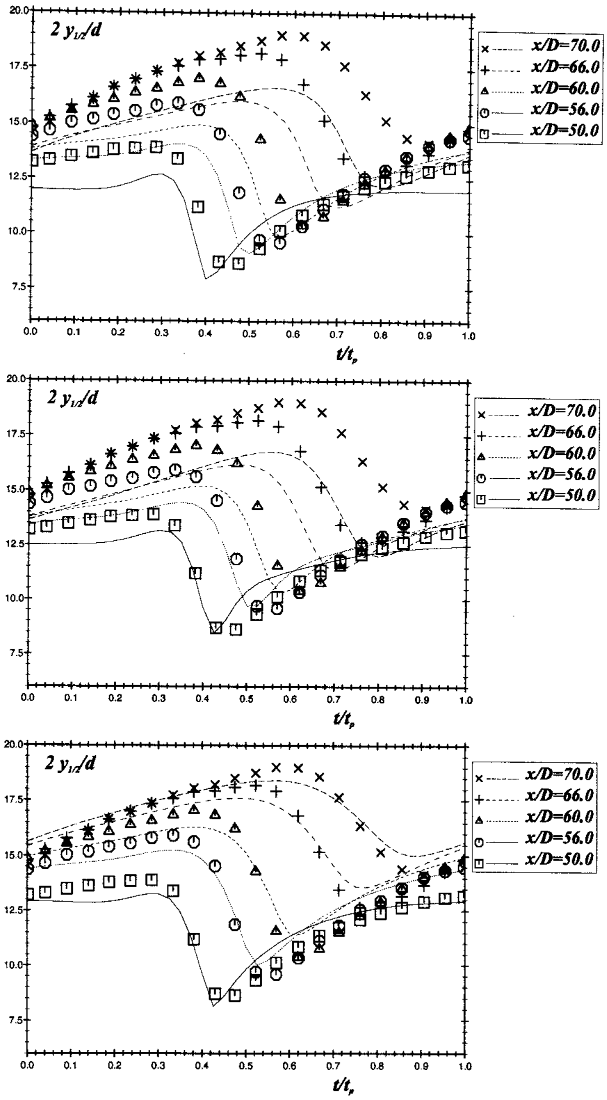

Figure 1: Jet half-width development through a pulsing cycle at various x/d positions. Top graph: k-ε model; Middle graph: TCL model; Bottom graph: HLS scheme; Lines: computations; Symbols: experiments of Bremhorst & Gehrke (2000).

Pulsed Jet at 10Hz

Turning attention to the pulsed jet, Figure 1 shows a comparison of the half-width growth through a pulsing cycle at a number of downstream distances reported by Bremhorst & Gehrke (2000). Both the k-ε and TCL predictions underestimate not only the difference between maximum and minimum half-widths through the cyle but also the growth of half-width with downstream distance (features also noted with other single-time-scale models tested). On the other hand, the two-scale model displays excellent agreement with the measurements.

The significant effect that the two-scale model has on the decay of centreline turbulent kinetic energy with downstream distance is shown in Figure 2. In the region of $x/d = 40-70$, the kinetic energy is maintained almost constant and at a much higher level than found for steady jets. This is again consistent with the measurements of Bremhorst & Gehrke, who reported a roughly constant level for k/U_o^2 of around 0.12 over this region, but is in contrast to the TCL and k-ε schemes which both predict a monotonic decrease of turbulence energy levels.

The two-scale model predictions of the averaged jet half-width as a function of downstream distance, shown in Figure 3, exhibit a distinct change of slope after about $x/d = 35$ which is also reflected in a change of the decay rate of centre-line velocity (Figure 4). Neither of these features is predicted by the single-time-scale models tested, but again the HLS computations result in good agreement with the experimental data.

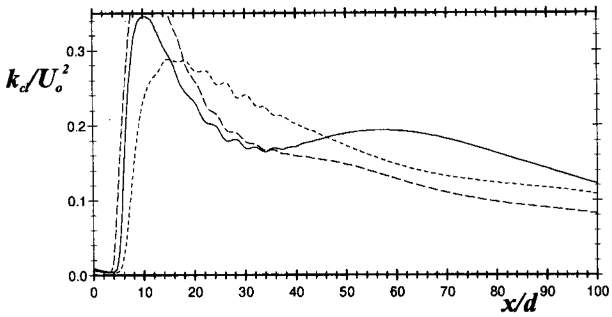

Figure 2: Decay of centreline turbulent kinetic energy averaged through a cycle. ——: HLS scheme; - - -: k-ε model; – –: TCL model.

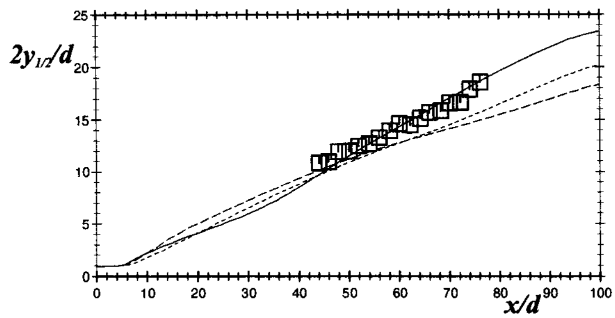

Figure 3: Development of averaged jet half-width. ——: HLS scheme; - - -: k-ε model; – –: TCL model; Symbols: experiments of Bremhorst & Gehrke (2000).

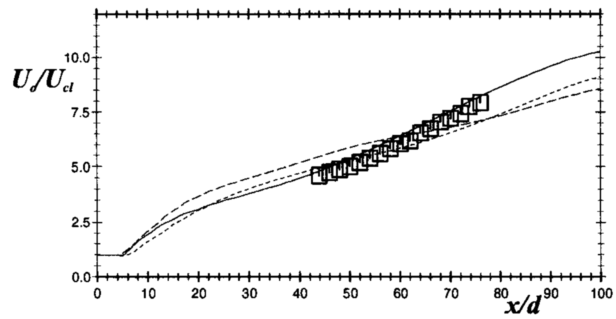

Figure 4: Decay of averaged centre-line velocity. ——: HLS scheme; - - -: k-ε model; – –: TCL model; Symbols: experiments of Bremhorst & Gehrke (2000).

Pulsed Jet at 80Hz

As a further test of the two-scale model, computations were performed at a higher pulsing frequency of 80Hz. Whereas in the 10Hz case the predictions showed the pulsing behaviour to extend for most of the domain length, at this higher frequency the region of pulse domination was much shorter, with the model predicting the jet to be essentially steady after a distance of around 30 diameters. As can be seen from Figure 5, at this higher frequency the model did not predict the kinks in spreading rate or centreline velocity decay seen previously, and returned generally lower centreline turbulence energy levels. Experimental data by Winter (1991), who reported measurements made at a variety of frequencies ranging from 20 to 160Hz, does support some of these observations (such as the absence of the mid-domain change in velocity decay rate at higher pulsing frequencies). However, they also show a general increase in the half-width growth as the frequency increases from 20 to 120 Hz, before it begins to fall again at even higher frequencies. This would not appear to be predicted by the present scheme, since Figure 5 shows that although the 80Hz jet initially begins to spread more rapidly than the 10Hz one, its growth rate then decreases at around $x/d = 30$, whilst that of the 10Hz jet increases.

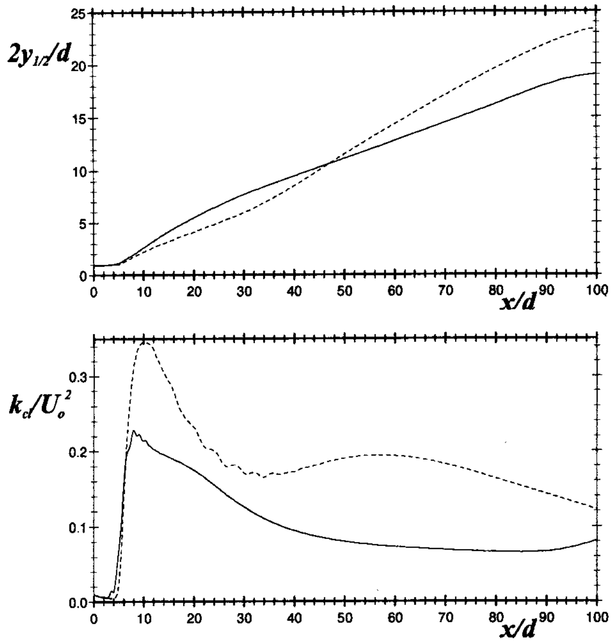

Figure 5: Development of averaged jet half-width and centreline turbulent kinetic energy, using the HLS model. ——: 80Hz case; - - -: 10Hz case.

MODELLING INVESTIGATIONS

In attempting to understand what aspects of the two-scale model brought about the good agreement with experiments in the 10Hz case, it is necessary to examine in more detail the two novel features which the scheme introduces: the partitioning of the turbulence spectrum and the non-equal weighting given to shear and normal straining through the combined action of the ε_P generation terms.

To shed some further light on the model's behaviour, Figure 6 shows the predicted values of k_P, k_T, ε_P and ε_T through a pulse at $x/d = 10$ and 50. As can be seen, over much of the flow the vast majority of the turbulence energy is contained in the production range, k_P, and except for some small differences in the early jet development stages the transfer and dissipation rates ε_P and ε_T take very similar values to each other. This would suggest that the effects of spectral non-equilibrium may not actually be the crucial feature of the model in this flow. Although this was initially a rather surprising result, given the quite significant differ-

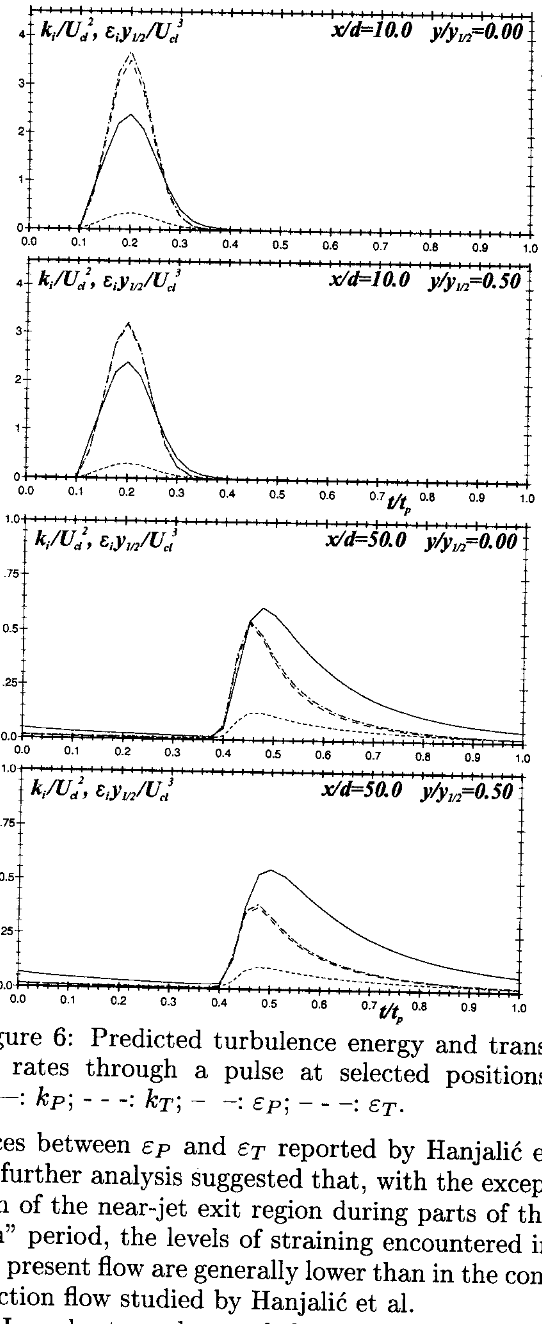

Figure 6: Predicted turbulence energy and transfer rates through a pulse at selected positions. ——: k_P; - - -: k_T; – –: ε_P; – – –: ε_T.

ences between ε_P and ε_T reported by Hanjalić et al, further analysis suggested that, with the exception of the near-jet exit region during parts of the "on" period, the levels of straining encountered in the present flow are generally lower than in the contraction flow studied by Hanjalić et al.

In order to understand the effect of the second feature noted in the Hanjalić et al scheme, namely the two generation mechanisms for ε_P, it is instructive to note that the second term, associated with the C'_{P1} coefficient, vanishes in irrotational strain, whilst in a simple shear the combined contribution is

$$k\left(\frac{dU}{dy}\right)^2\left[0.09C_{P1} + C'_{P1}\frac{k_P}{k}\right] \qquad (9)$$

Since C'_{P1} is negative, in an equilibrium shear flow the combined contribution effectively reduces to the usual source term employed in a standard k-ε scheme. However, in irrotational straining the second term vanishes, resulting in a much larger overall source than would be present in a standard ε equation. To examine the contribution of this model feature in the pulsed jet, a further calculation was performed using values of

$$C_{P1} = 2.2 - \frac{0.11}{0.09}\frac{k_P}{k} \qquad C'_{P1} = 0 \qquad (10)$$

which effectively leaves a source term with equal weighting for shear and normal straining. Predictions of the steady axisymmetric jet with this modified source term are similar to those of the original HLS scheme reported in Table 2. However, Figure 7 shows that when applied to the pulsed jet, the modification leads to a significant deterioration in the prediction of the half-width growth. The importance of the mixed generation term is further highlighted by Figure 8, where the modified scheme is seen to return a low averaged half-width growth and, although producing a higher initial peak level of centreline turbulence energy, the plateau seen with the original model between $x/d = 40$ and 70 is no longer present. Computations with different values of C_{P1} and C'_{P1} showed that small changes from the values proposed by Hanjalić et al lead to significant changes in the magnitude and phase of quantities through the pulsing cycle, thus suggesting that the original values are near optimal.

One question which naturally arises from the above investigations is whether a single-scale model which employed the mixed generation term of equation (5) would also perform well in the pulsed jet case. Initial efforts at including both terms within an otherwise standard k-ε scheme did not, however, produce any stable solutions. Further tests were also performed with the model proposed by Hanjalić & Launder (1980), which is a linear single-scale scheme employing a similar combination of source terms in the ε equation. However, this was also found to be numerically unstable in the present flows, particularly in the pulsed case. These instabilities originated at the very outer edge of the jet, where there is a fairly complex balance between convection, generation, destruction and diffusion terms, and where, because of the low turbulence levels, small changes in some model coefficients can result in significantly different turbulent timescales.

Further investigations of the two-scale model

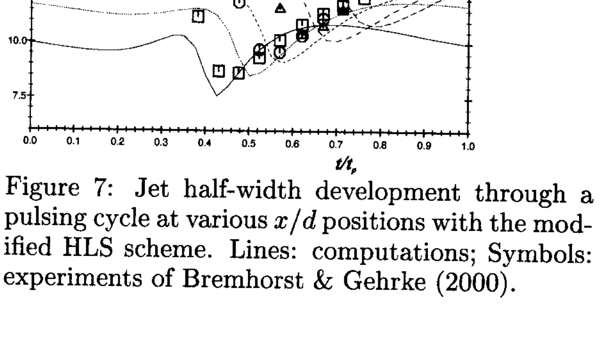

Figure 7: Jet half-width development through a pulsing cycle at various x/d positions with the modified HLS scheme. Lines: computations; Symbols: experiments of Bremhorst & Gehrke (2000).

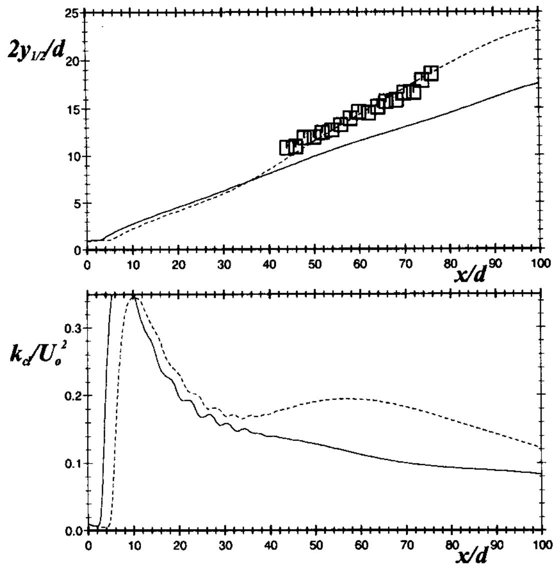

Figure 8: Averaged jet half-width and centreline turbulence energy. ——: HLS scheme with modified ε_P source term; - - -: HLS scheme; Symbols: exp. of Bremhorst & Gehrke (2000).

also underlined the importance of ensuring a careful balance of terms at the outer edge of the jet: a reduction in the turbulent diffusion of ε_P, for example, also resulted in numerical instabilities arising from the imbalance of turbulence quantities at the outer edge of the jet. Interestingly, one feature of the Mataoui et al (2001) two-scale model, referred to earlier, is that it employs a much higher turbulent Prandtl number for ε_T than for other quantities. Such a decrease in the diffusion of ε_T in the present scheme leads to a reduction in the change of centreline velocity decay slope where the jet changes from pulse domination to steady behaviour. These observations suggest that the diffusion process is not only crucial in ensuring numerical stability, but is also an essential part of the spectral transfer process, even in the transfer range.

CONCLUSIONS

The two-scale HLS scheme was the only model tested that was found to reproduce many of the features of the 10Hz pulsed jet flow. Further investigations suggest that much of this improvement (although not all) is achieved via the source terms in the ε_P equation, which show a stronger response to normal straining than shearing. However, even this model did not entirely capture the measured changes in jet behaviour at different pulsing frequencies, and further investigations of the model source terms and turbulence spectrum distributions in these cases is needed. Another avenue of investigation to be pursued will be to incorporate some of the above modelling approaches within non-linear EVM and stress transport schemes, which can be expected to return significantly better stress anisotropy levels when applied to more complex flows.

Authors' names appear alphabetically.

REFERENCES

Bremhorst, K., Harch, W.H., 1979, "Near field velocity measurements in a fully pulsed subsonic air jet", *Turbulent Shear Flows 1* (eds. F. Durst, B.E. Launder, F.W. Schmidt, J.H. Whitelaw), Springer-Verlag.

Bremhorst, K., Gehrke, P.J., 2000, "Measured Reynolds stress distributions and energy budgets of a fully pulsed round air jet", *Expts. in Fluids*, **28**, 519-531.

Craft, T.J., Ince, N.Z., Launder, B.E., 1996, "Recent developments in second-moment closure for buoyancy-affected flows", *Dynamics of Atmospheres and Oceans*, **23**, 99-114.

Craft, T.J., Launder, B.E., 2001, "Principles and performance of TCL-based second-moment closures", *Flow, Turb. & Combustion*, **66**, 355-372.

Graham, L.J.W., Bremhorst, K., 1993, "Application of the k-ε turbulence model to the simulation of a fully pulsed free air jet", *Trans. ASME J. of Fluids Eng.*, **115**, 70-74.

Hanjalić, K., Launder, B.E., Schiestel, R., 1980, "Multiple-time-scale concepts in turbulent transport modelling", *Turbulent Shear Flows 2* (eds. L.J.S. Bradbury, F. Durst, B.E. Launder, F.W. Schmidt, J.H. Whitelaw), Springer-Verlag.

Hanjalić, K., Launder, B.E., 1980, "Sensitizing the dissipation equation to irrotational strains", *Trans. ASME J. of Fluids Eng.*, **102**, 34-40.

Launder, B.E., Li, S-P., 1994, "On the elimination of wall-topography parameters from second-moment closure", *Phys. Fluids*, **6**, 999-1006.

Lien, F-S., Leschziner, M.A., 1994, "A general non-orthogonal finite-volume algorithm for turbulent flow at all speeds incorporating second-moment turbulence-transport closure", *Comp. Meth. Appl. Mech. Eng.*, **114**, 123-167.

Leschziner, M.A., Lien, F-S., 1994, "Upstream monotonic interpolation for scalar transport with application to complex turbulent flows", *Int. J. for Numerical Methods in Fluids*, **19**, 527-548.

Mataoui, A., Schiestel, R., Salem, A., 2001, "Flow regimes of interaction of a turbulent plane jet into a rectangular cavity: experimental approach and numerical modelling", *Flow, Turb. & Combustion*, **67**, 267-304.

Nordsveen, M., Bremhorst, K., 1998, "Simulations of a fully pulsed round turbulent air jet flow with k-ε and Reynolds stress turbulence models", *Proc. 13th Australasian Fluid Mechanics Conference*, Monash University, Melbourne, Australia.

Rhie, C.M., Chow, W.L., 1983, "Numerical study of the turbulent flow past an airfoil with trailing edge separation", *AIAA J.*, **21**, 1525-1532.

Winter, A.E., 1991, "A laser Doppler anemometer investigation into fully pulsed jet flows with an examination of velocity bias errors", PhD Thesis, The University of Queensland, Australia.